REGOLITH THICKNESS ESTIMATION OVER SINUS IRIDUM USING MORPHOLOGY AND SIZE-FREQUENCY DISTRIBUTION OF SMALL CRATERS FROM LROC IMAGES. Tiantian Liu[1], Wenzhe Fa[1], Menghua Zhu[2], and Junichi Haruyama[3], [1]Institute of Remote Sensing and Geographical Information System, Peking University, Beijing, China (wzfa@pku.edu.cn). [2]Space Science Institute, Macau University of Science and Technology, Macau, China. [3]Institute of Space and Astronautical Science, Japan Aerospace Exploration Agency, Japan.

Introduction: Knowledge of lunar regolith thickness provides important information for scientific questions about the evolution of lunar surface and engineering constrains for lunar explorations. The major methods for regolith thickness estimation include in situ geophysical measurements [1], remote sensing techniques at radio frequency [2-5], and morphology and size-frequency distribution of small fresh craters [6]. Based on these methods, it is now recognized that typical regolith thickness is about 4-5 m over maria and 10-15 m in the older highland region [2]. However, there are still large uncertainties in the estimated regolith thickness over local regions, for example, the Sinus Iridum region [2-5].

Recently, the release of high-resolution optical images from Lunar Reconnaissance Orbiter Camera (LROC) Narrow Angle Cameras (NACs) makes it possible to estimate regional regolith thickness with a high precision using morphology of small craters [7]. In this study, regolith thickness over the Sinus Iridum region is estimated using morphology and size-frequency distribution of small impact craters from LROC NAC images. Statistical characteristics and local variation of regolith thickness and its correlation with surface age are discussed. The same approach can be applied to regolith thickness estimation over China's Chang'E-3 (CE-3) landing site, which can help to analyze CE-3 ground penetrating radar (GPR) echoes.

Regolith Thickness Estimation Approach: High-resolution photographs from Lunar Orbiter (LO) showed that morphologies of small fresh craters can be classified into three types: normal, flat-bottomed, and concentric (Fig. 1). Extensive laboratory experiments by impacting projectiles against targets consisting of loose materials overlying more cohesive substrates showed that the same types of craters can be produced and morphologies of small craters depend mainly on the thickness of the surficial layer [6]. It was found that when regolith layer is thicker than a value between D_A/3.8 and D_A/4.2, normal craters form, and concentric craters form when regolith layer is thinner than a value between D_A/8 and D_A/10, where D_A is the rim-to-rim diameter of the final crater [6]. By assuming that distributions of the various morphologic types of craters are uniform, cumulative distribution of regolith thickness can be obtained from size-frequency distribution of small impact craters.

Based on the old experimental data [6], a revised relationship between crater geometry and regolith thickness is proposed as

$$D_F/D_A = 0.834(\pm 0.067) - \frac{1.875\cot 31^\circ}{D_A/d} \qquad (1)$$

where D_F is the diameter of the floor of flat-bottomed and concentric craters, and d is regolith thickness. The constant after +/- corresponds to the upper/lower envelope that encloses the experimental data. Since normal (concentric) craters constrain the lower (upper) limit of regolith thickness, the upper envelope curve gives rise to a thicker regolith with a lower (higher) confidence level, whereas the lower envelope results in a smaller regolith thickness with a higher (lower) confidence level.

When regolith thickness over large region is of interest, multiple LROC NAC images with varying observation conditions have to be utilized. When illumination angle is smaller than repose angle of the regolith, a flat-bottomed crater could be misidentified as a normal crater, and a concentric crater could be misrecognized as a flat-bottomed one. In such a case, the experimental relation between crater geometry and regolith thickness should be revised. This can be obtained by considering an extreme case when the shadow cast by the crater rim completely covers the floor of a flat-bottomed crater, and when the shadow cast by the rim of the outer crater just touches the rim of the inner crater for a concentric crater (as discussed in more detail in section 5 of [6]). Combined the modified separating boundary with equation (1), the effect of illumination angle can be taken into account.

Regolith Thickness Results: Sinus Iridum (45.01°N, 31.67°W; 249.29 km diameter) is a bay of basaltic lava on the northwest of Mare Imbrium (Fig. 2) [8]. According to Hiesinger et al. [9], the surface was divided into four geologic units as I11, I17, I21 and I22, with their surface ages of 3.39, 3.26, 3.01 and 2.96 b.y., respectively. In this study, 264 LROC NAC images with spatial resolutions ranging from 0.34 to 1.81 m and illumination angles from 15° to 51° were selected. Totally, 379214 small fresh craters are counted, of which 275090 are normal craters with diameters between 4.2 m and 99.4 m, 19156 are flat-bottomed craters with diameters between 9.3 m and 234.6 m, and 84968 are concentric craters with diameters between

6.9 m and 249.8 m. Relative distributions of the counted craters show that normal craters dominate as diameters smaller than 35 m, and most of fresh craters with diameters larger than 100 m are concentric.

By using the revised relation and information of the counted craters, Fig. 3 shows the spatial distribution of the median regolith thickness estimated from normal (left column) and concentric (right column) craters for the studying region with a higher (upper row) and a lower (lower row) confidence level. As can be seen, median regolith thickness estimated from normal craters varies from 6 to 14 m with a mean value of 9 m, and that estimated from concentric craters varies from 3 to 14 m with a mean value of 5.9 m. Compared the left column with the right column, the overall distribution trend of regolith thickness can be displayed in the estimations from normal craters, whereas local variations of regolith thickness are highlighted in the results estimated from concentric craters. Analysis shows that regolith thickness estimated from normal (concentric) craters for regions A, B, and C in Fig. 2 are 1.9 (0.8), 1.2 (0.4) and 3.4 (1.2) m larger than their background geologic units, respectively.

Fig. 4a shows the cumulative distribution of regolith thickness estimated from normal (red) and concentric (blue) craters. On the basis of normal (concentric) craters, regolith thickness is estimated to be from 2 to 24 m, with a median value of 9.1 (5.0) m. Regolith thickness of 25% region is smaller than 6.2 (3.2) m, and 75% of the region is with thickness thinner than 12 (9) m based on normal (concentric) craters.

Fig. 4b shows the plot of regolith thickness versus surface age for the four geologic units (Fig. 2) estimated from normal craters. The median regolith thicknesses are 9.6, 9.4, 8.5 and 7.6 m for the geologic units I11, I17, I21, and I22, respectively. There is a strong correlation between the median regolith thickness and surface age: the older the surface, the thicker the regolith. The average regolith growth rate is estimated to be ~4.65 m/b.y..

Conclusions and Future Work: Using morphology and size-frequency distribution of small impact craters from LROC images, local variation of regolith thickness and its correlation with surface age over the Sinus Iridum region are investigated. Our results show that median regolith thickness in Sinus Iridum is between 5 m and 9.1 m, and most of the region is with thickness smaller than 12 m. We are now applying the same approach to study the regolith thickness over CE-3 landing site, which will help to decipher the GPR echoes.

References: [1] Nakamura Y. et al. (1975) *Moon*, *13*, 57–66. [2] Shkuratov Y. G. and Bondarenko N. V. (2001) *Icarus*, *149(2)*, 329–338. [3] Chen S. et al. (2010) *Science China Physics Mechanics & Astronomy*, *53*, 2179–2187. [4] Kobayashi T. et al. (2010) *IEEE Geosci. and Remote Sen. Lett.*, *7*, 435–439. [5] Fa W. and Jin Y.-Q. (2010) *Icarus*, *207(2)*, 605–615. [6] Quaide W. L. and Oberbeck V. R. (1968) *JGR*, *73(16)*, 5247–5270. [7] Robinson M. S. et al. (2010) *Space Sci. Rev.*, *150*, 81–124. [8] Schaber G. G. (1969) *US Geological Survey*. [9] Hiesinger H. R. (2000) *JGR*, *105(E12)*, 29239–29275.

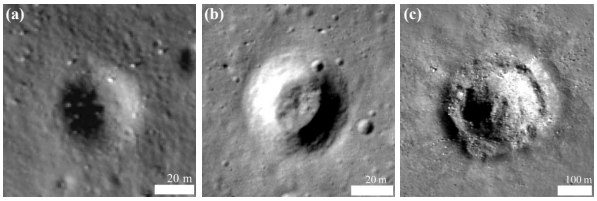

Figure 1. Examples of lunar craters with (a) normal, (b) flat-bottomed, and (c) concentric geometry.

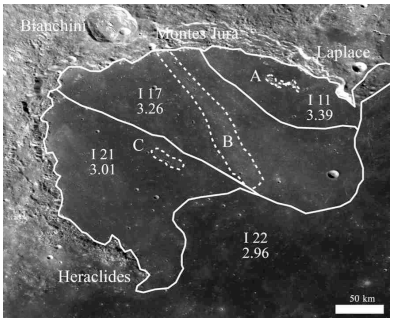

Figure 2. Geologic location of the Sinus Iridum region.

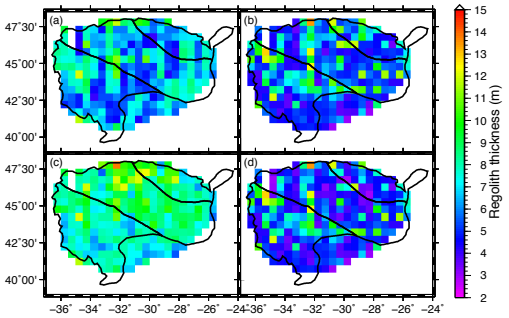

Figure 3. Distributions of median regolith thickness over the Sinus Iridum region.

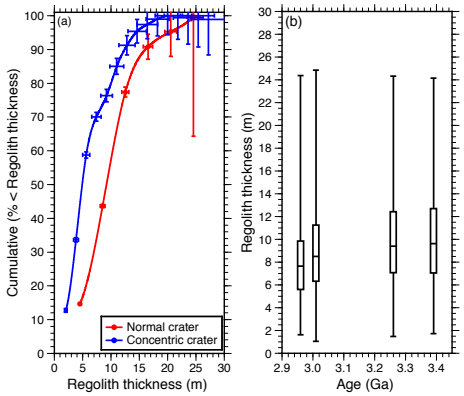

Figure 4. (a) Cumulative distribution of regolith thickness over the Sinus Iridum region. (b) The plot of regolith thickness versus surface age.